Electronic Supplementary Material (ESI) for Dalton Transactions.

Supporting Information for:

Recyclable Chemosensor for Oxalate Based on Bimetallic Complexes of a Dinucleating Bis(iminopyridine) Ligand

Jeffrey W. Beattie, David S. White, Amarnath Bheemaraju, Philip D. Martin, and Stanislav Groysman*

Department of Chemistry, Wayne State University, Detroit, Michigan 48202

Index *Page*

1. ^{1}H and ^{13}C NMR spectra S2-S5
2. Mass spectra S6-S17
3. X-ray crystallographic details S18-S19
4. UV-vis spectra S20-S29
5. Determination of binding constant S30-32
6. References S33

1. ^{1}H and ^{13}C NMR Spectra

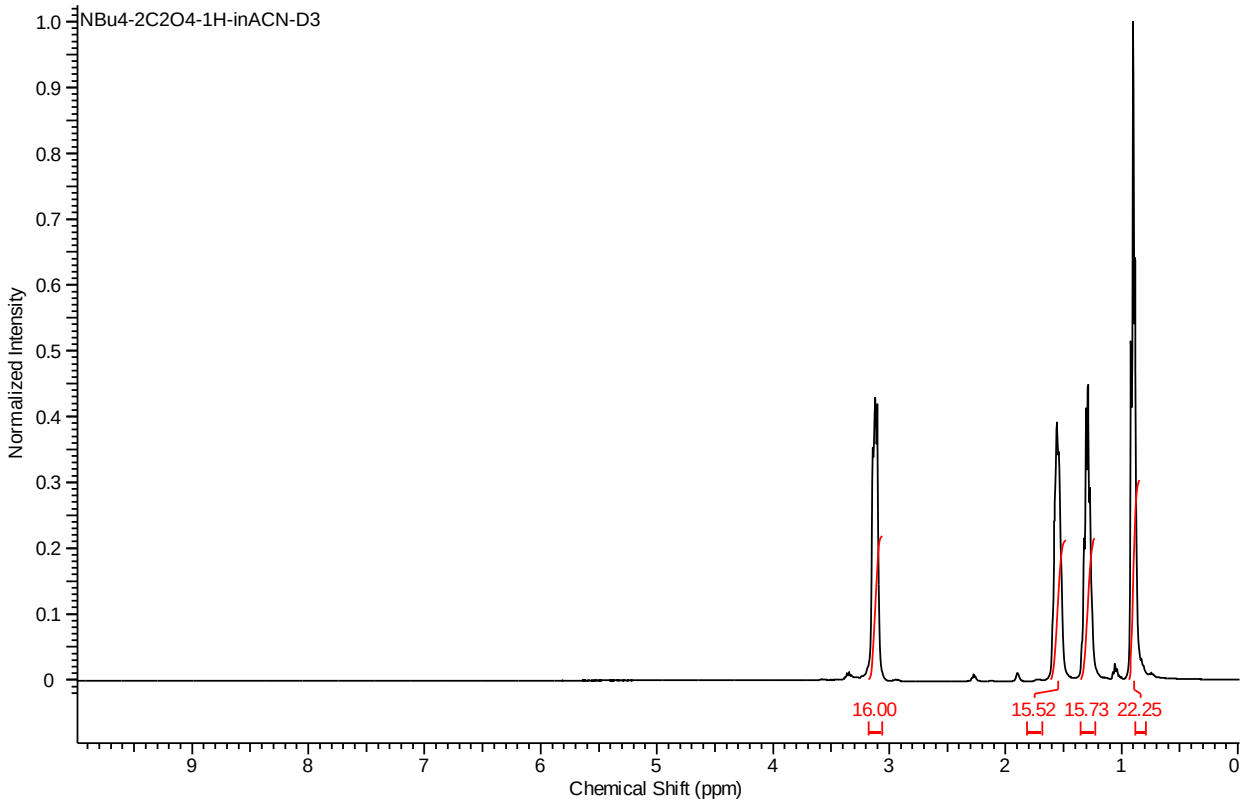

Figure S1. ^{1}H NMR spectrum of **$(NBu_4)_2[C_2O_4]$** in CD_3CN

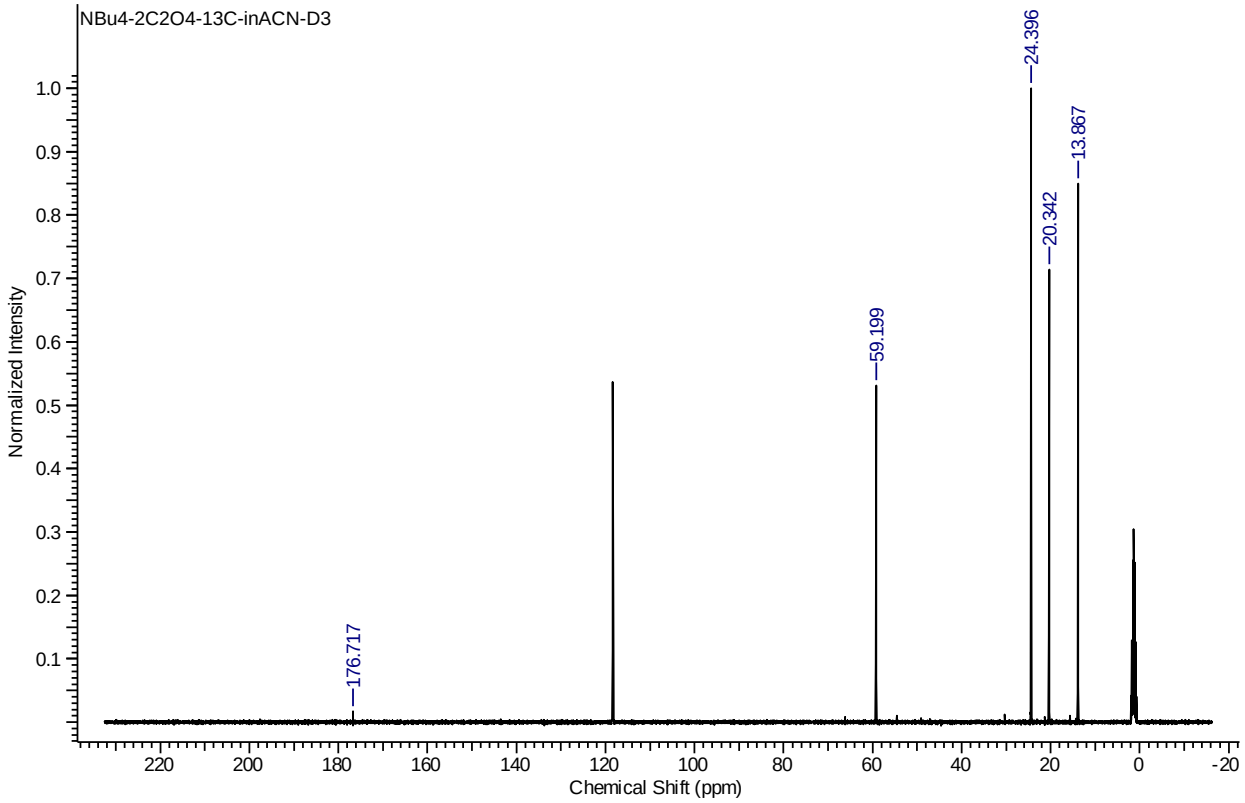

Figure S2. ^{13}C NMR spectrum of **$(NBu_4)_2[C_2O_4]$** in CD_3CN

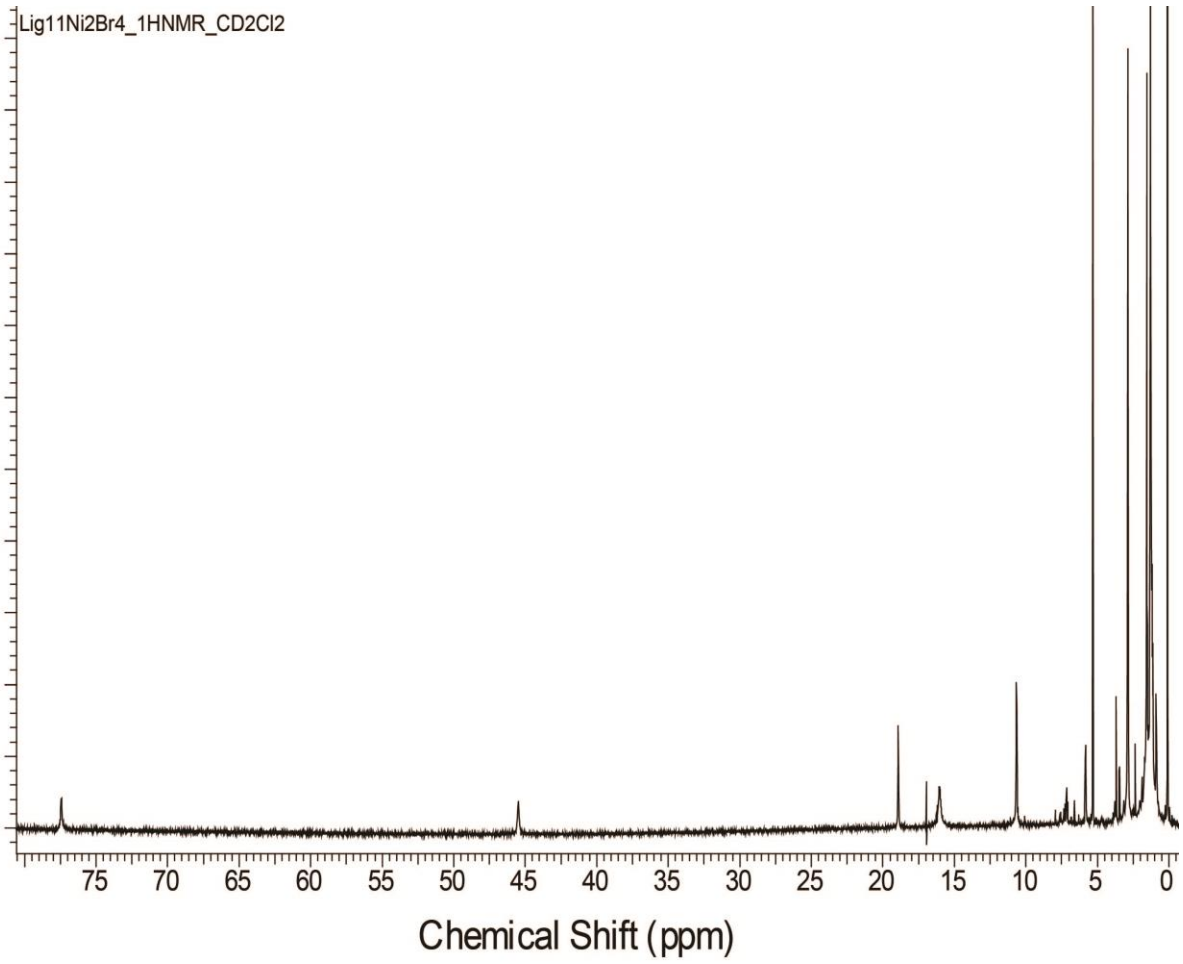

Figure S3. ^{1}H NMR spectrum of **1** in CD_2Cl_2. The spectrum was collected on the +100 to -100 ppm window; only the area that contains resonances is shown.

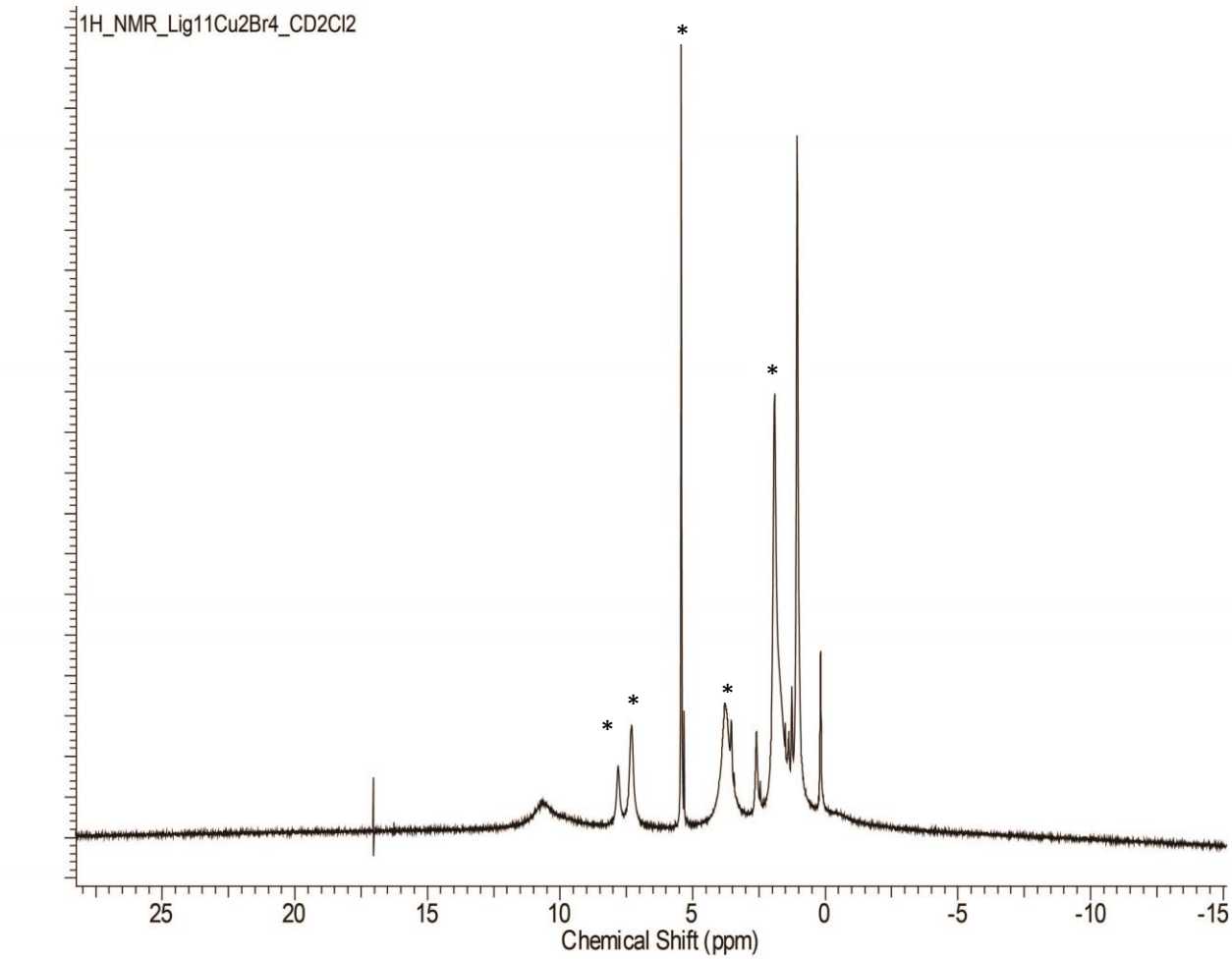

Figure S4. ^{1}H NMR spectrum of **2** in CD_2Cl_2. The spectrum was collected on the +100 to -100 ppm window; only the area that contains resonances is shown. Peaks marked by an asterisk are assigned to solvents (toluene, THF)

2. Mass Spectrometry

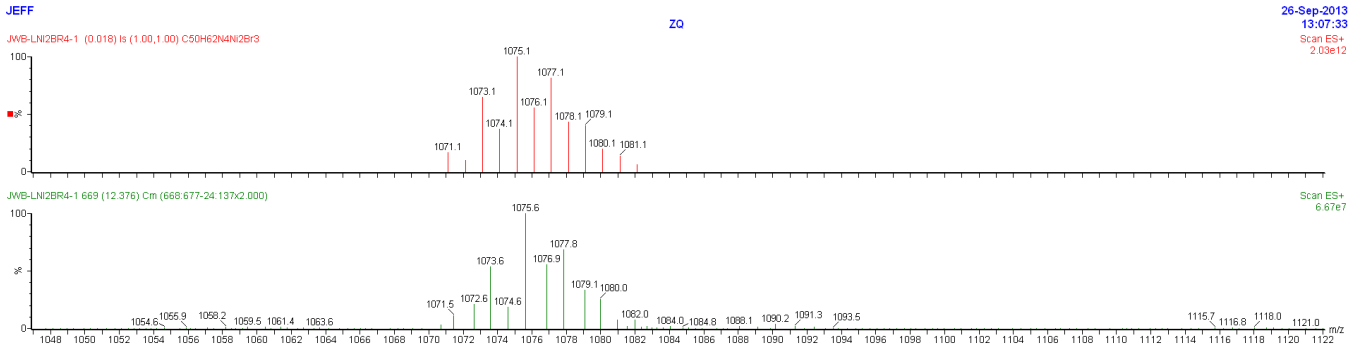

Figure S5. ESI-MS of **1**. The peak corresponding to $(\mathbf{1} - Br)^+$ is shown (below), along with the theoretical prediction of the isotopic distribution (top)

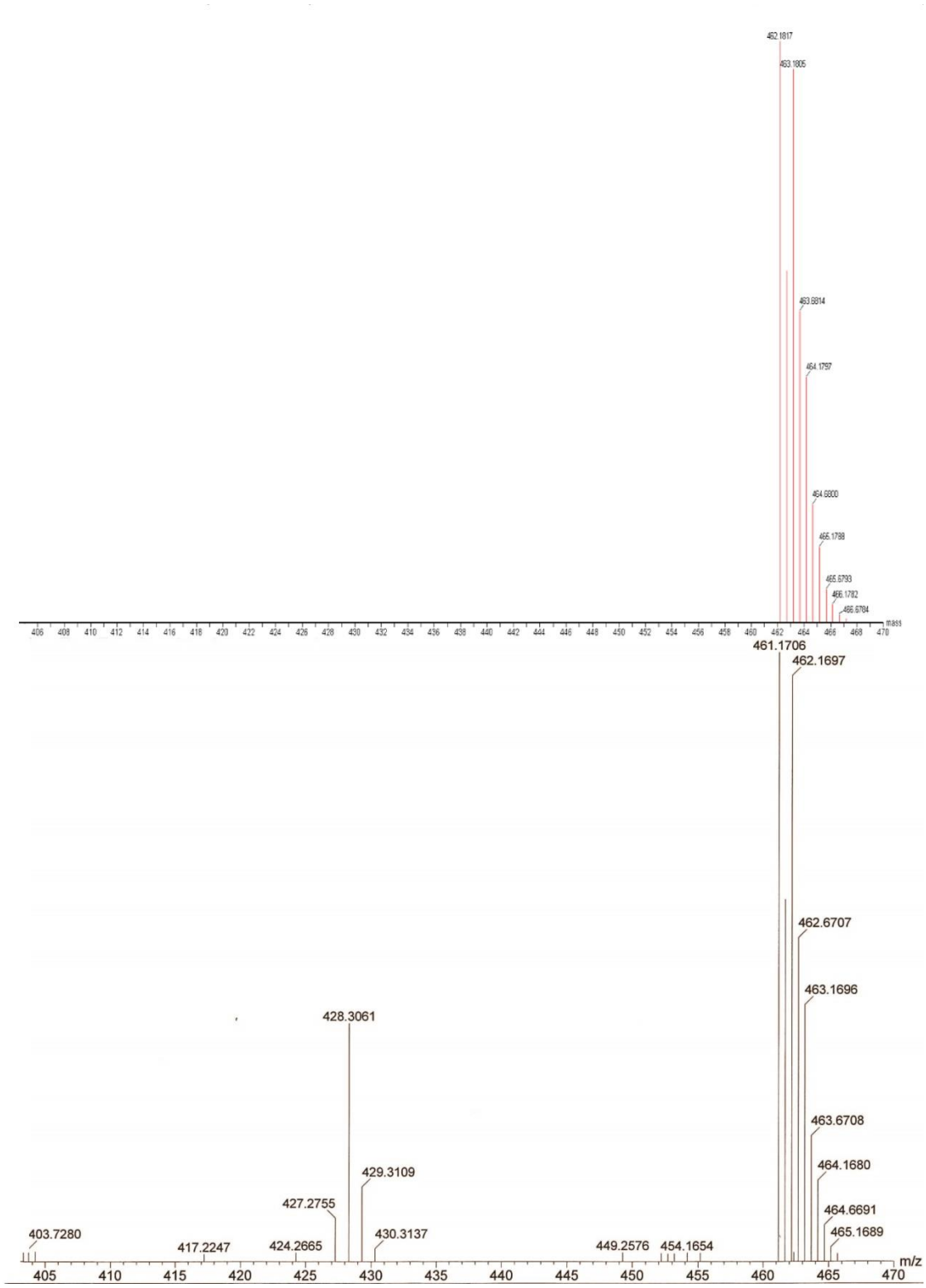

Figure S6. ESI-MS of **3**. The peak corresponding to $[\mathbf{3} - 2Br]^{2+}$ is shown (below), along with the theoretical prediction of the isotopic distribution (top)

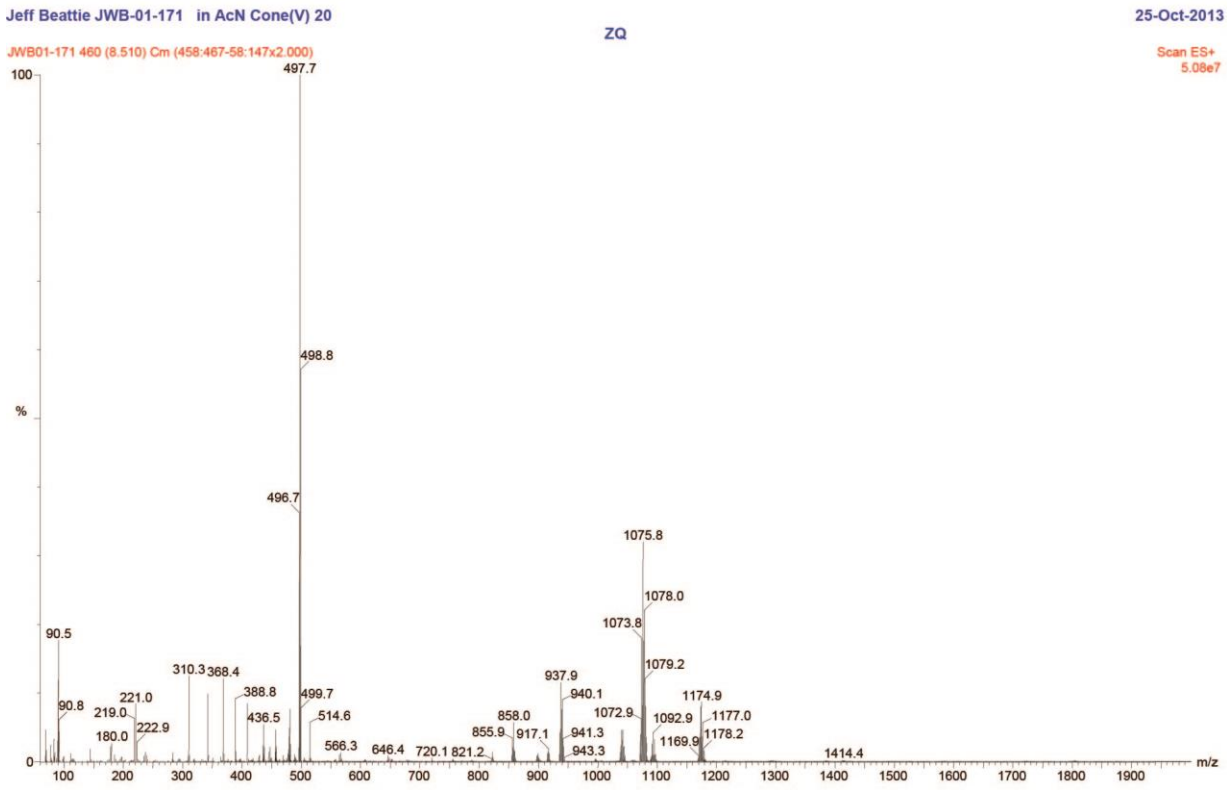

Figure S7. ESI-MS of **$Ni_2(L)Br_4$ + Formate**.

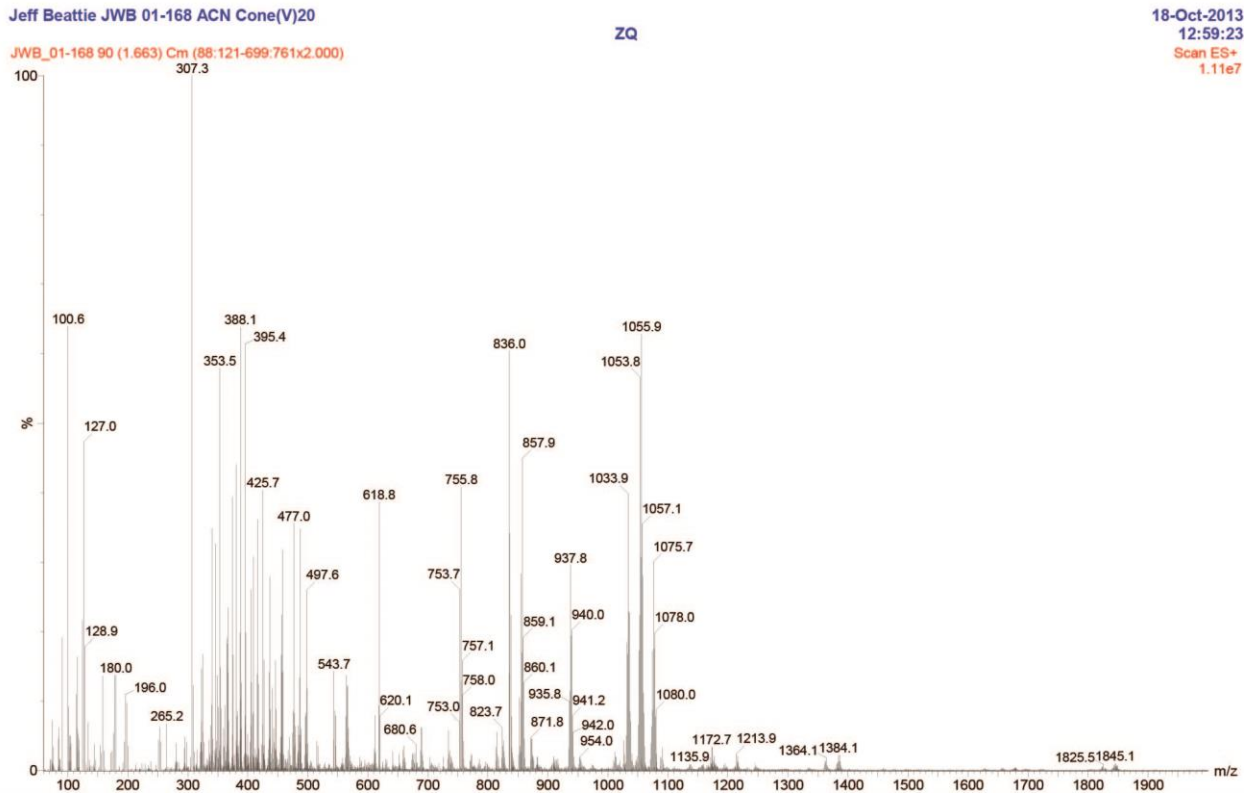

Figure S8. ESI-MS of **$Ni_2(L)Br_4$ + Acetate**

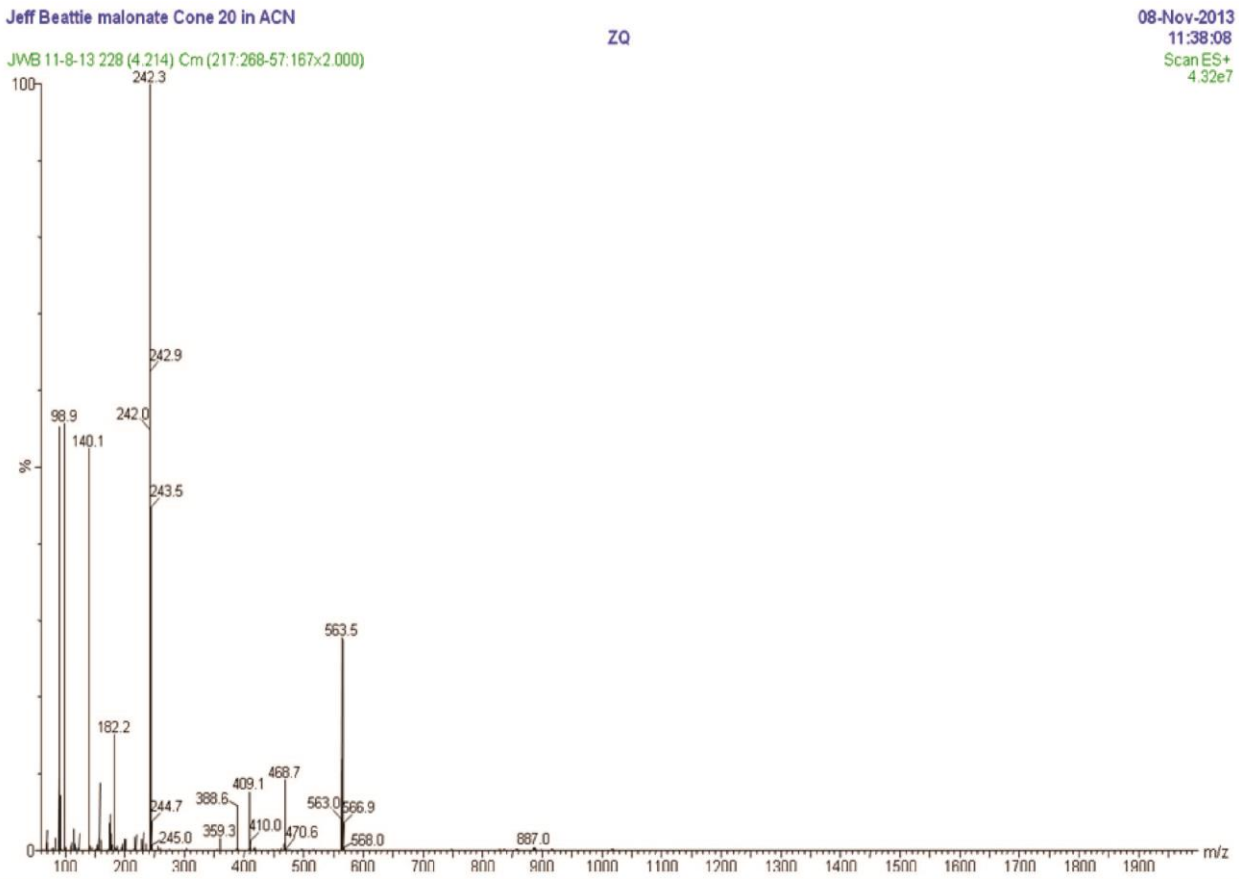

Figure S9. ESI-MS of **$Ni_2(L)Br_4$ + Malonate**

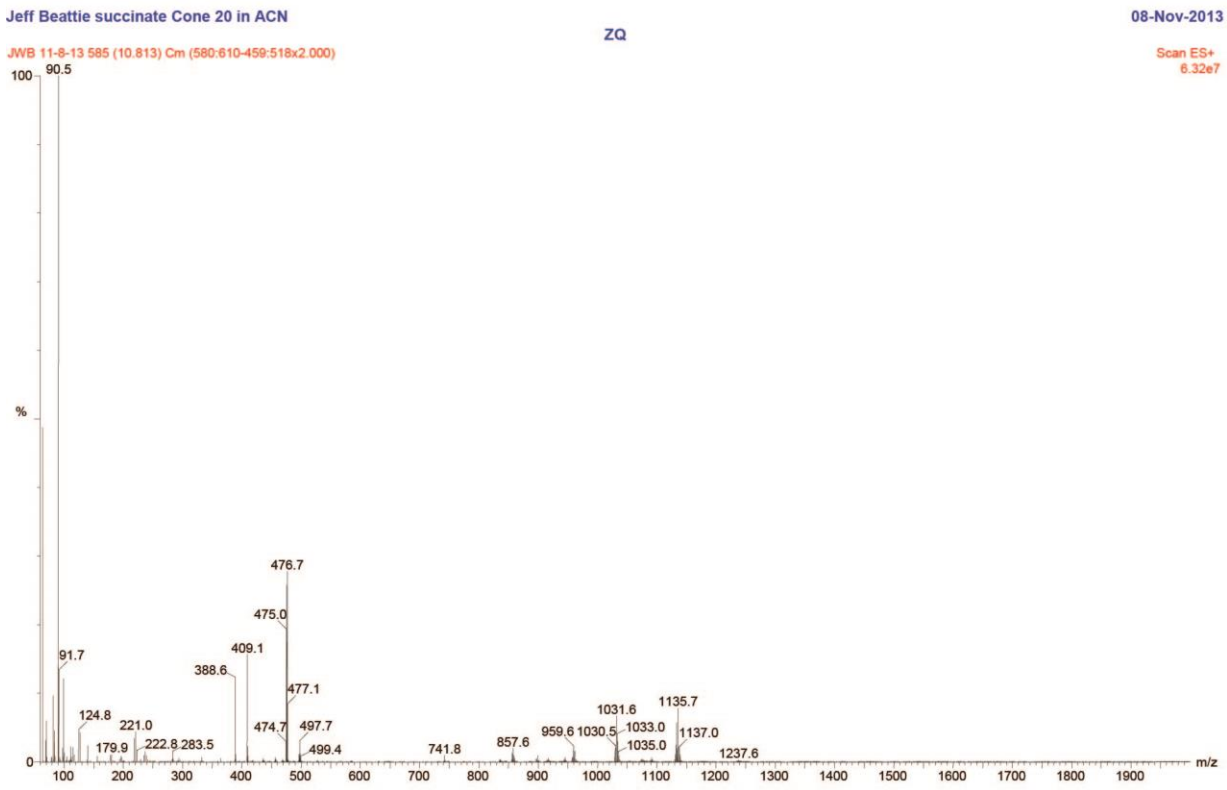

Figure S10. ESI-MS of **$Ni_2(L)Br_4$ + Succinate**

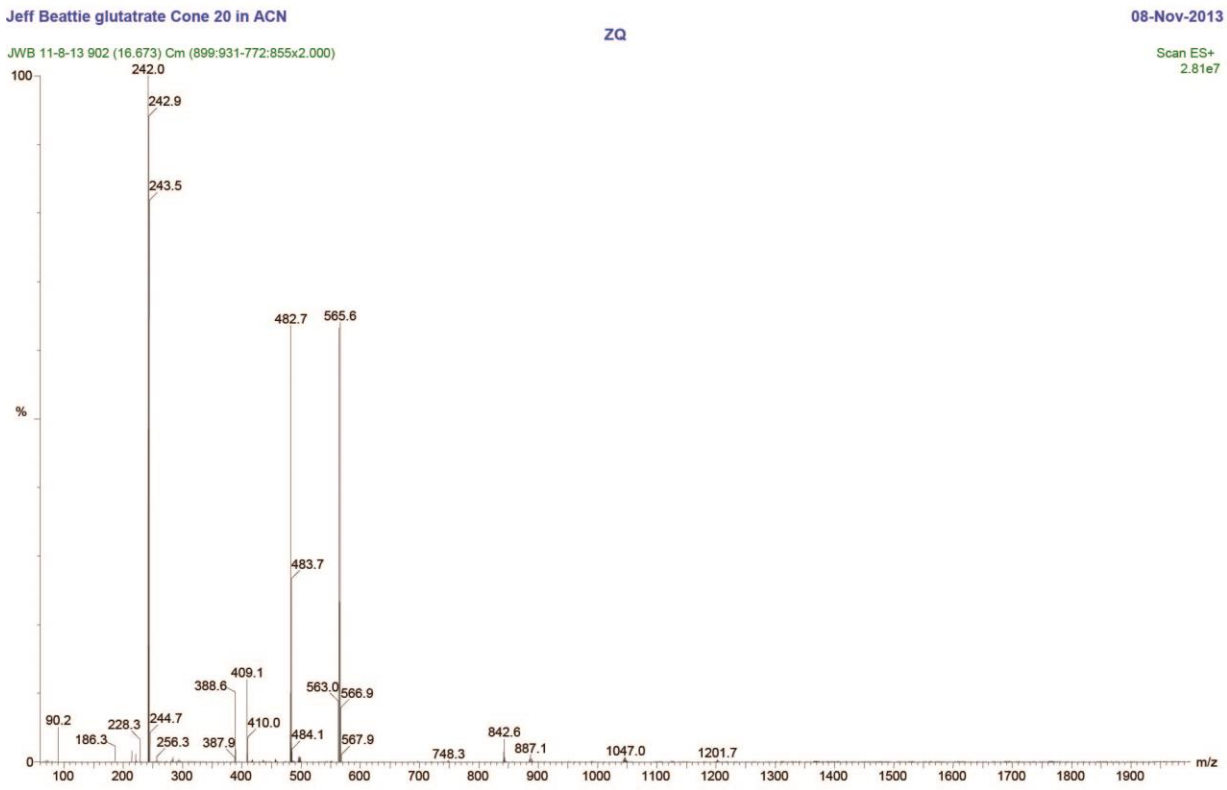

Figure S11. ESI-MS of **$Ni_2(L)Br_4$ + Glutarate**

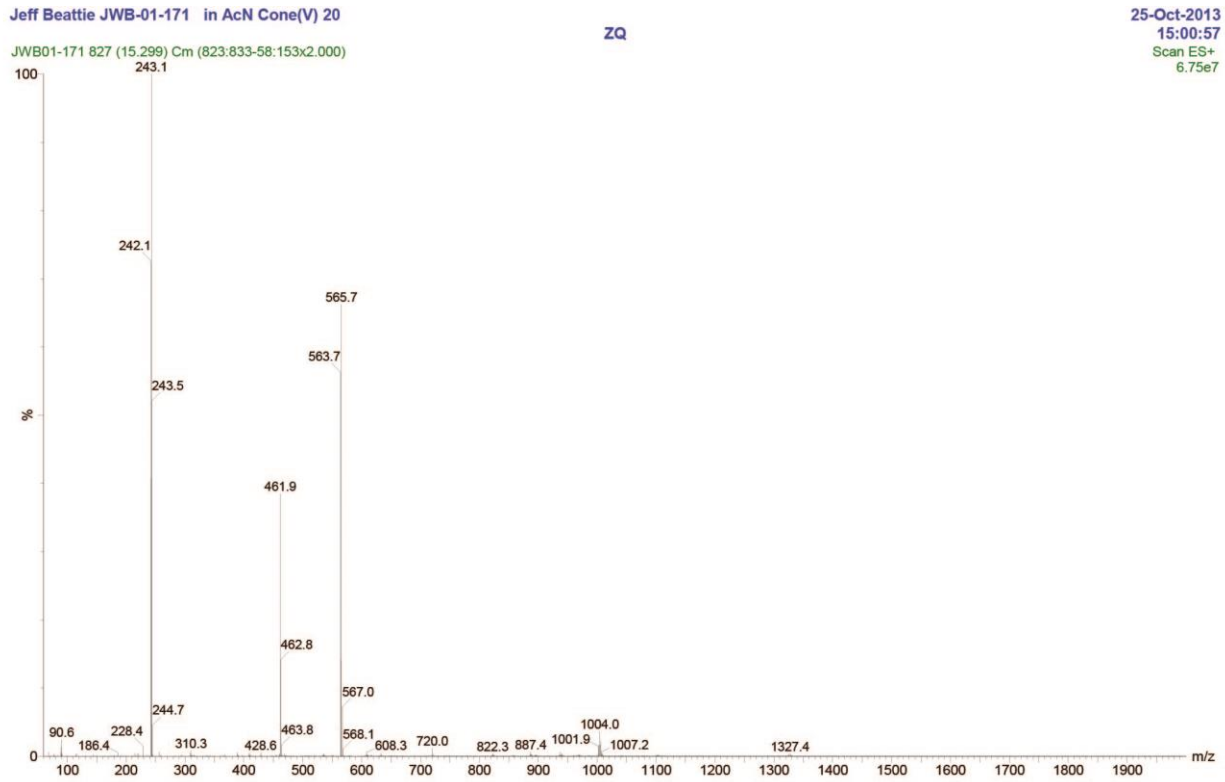

Figure S12. ESI-MS of **$Ni_2(L)Br_4$ + Formate** and **Oxalate**

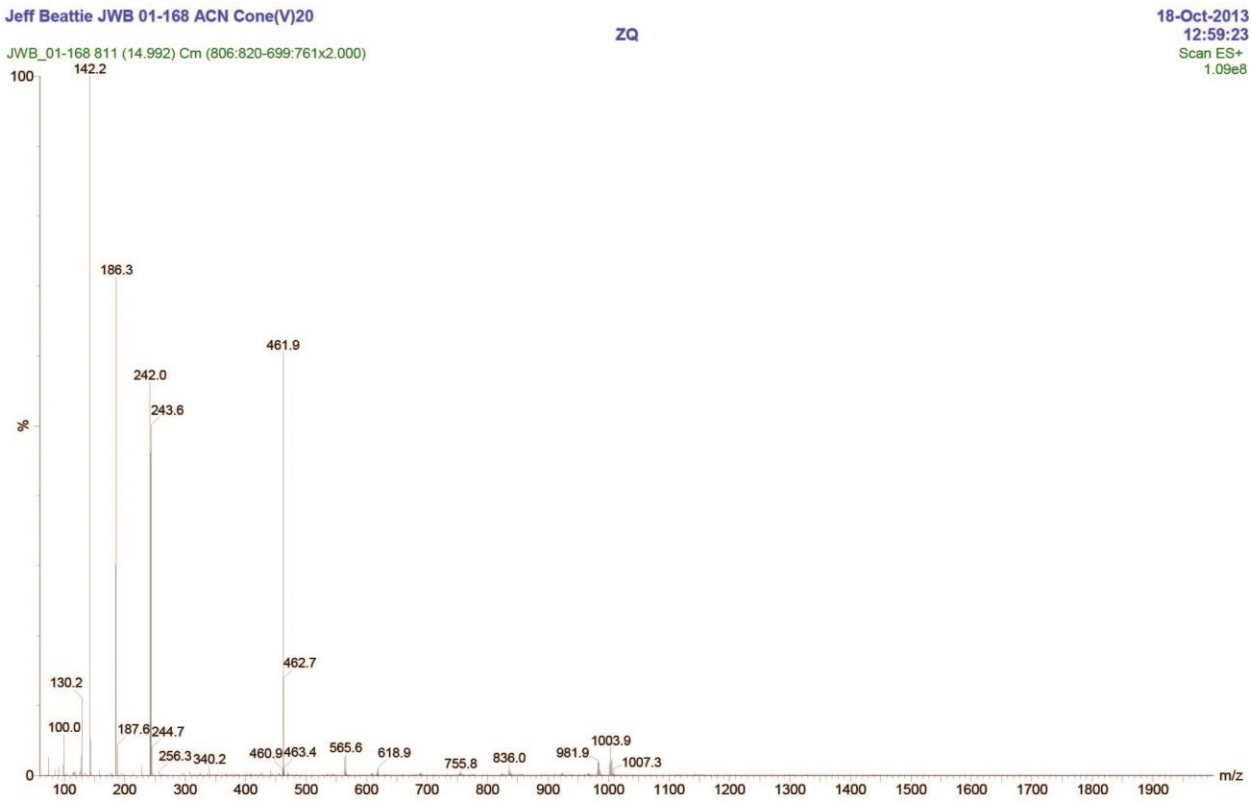

Figure S13. ESI-MS of **$Ni_2(L)Br_4$ + Acetate** and **Oxalate**

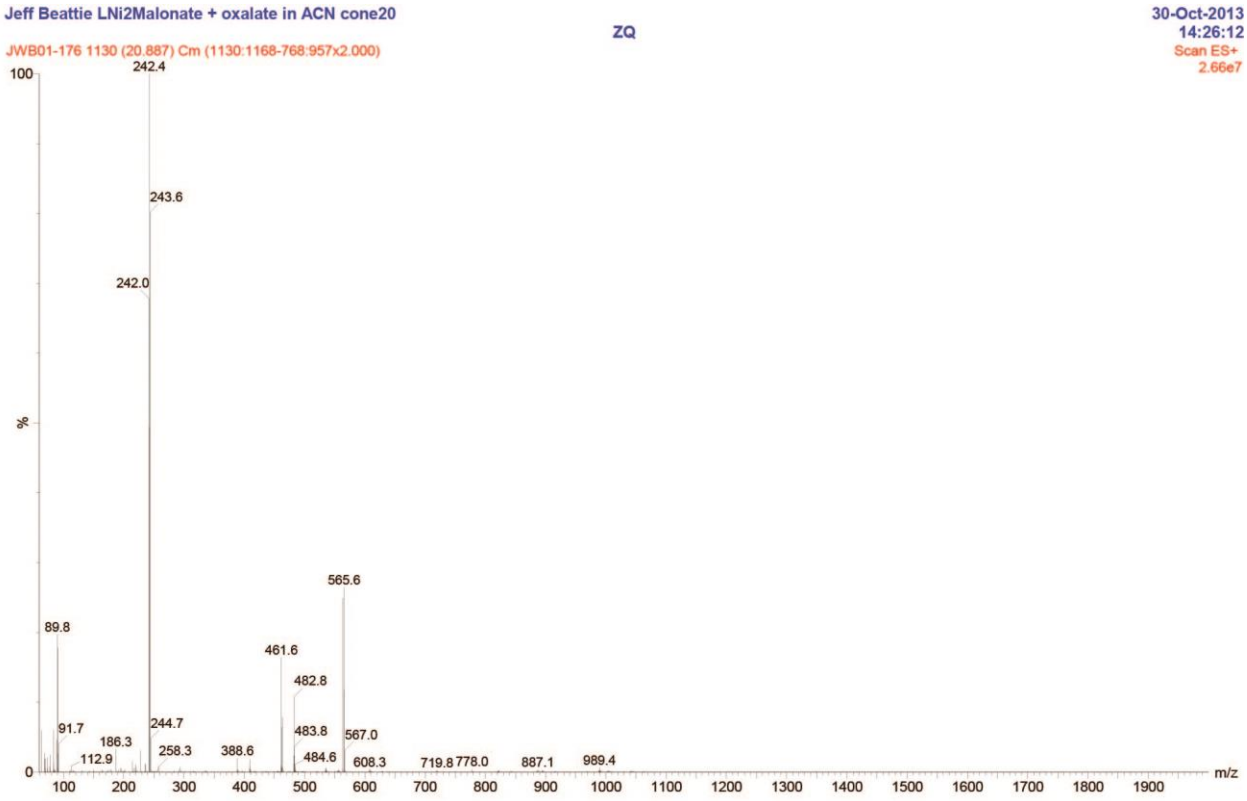

Figure S14. ESI-MS of **$Ni_2(L)Br_4$ + Malonate** and **Oxalate**

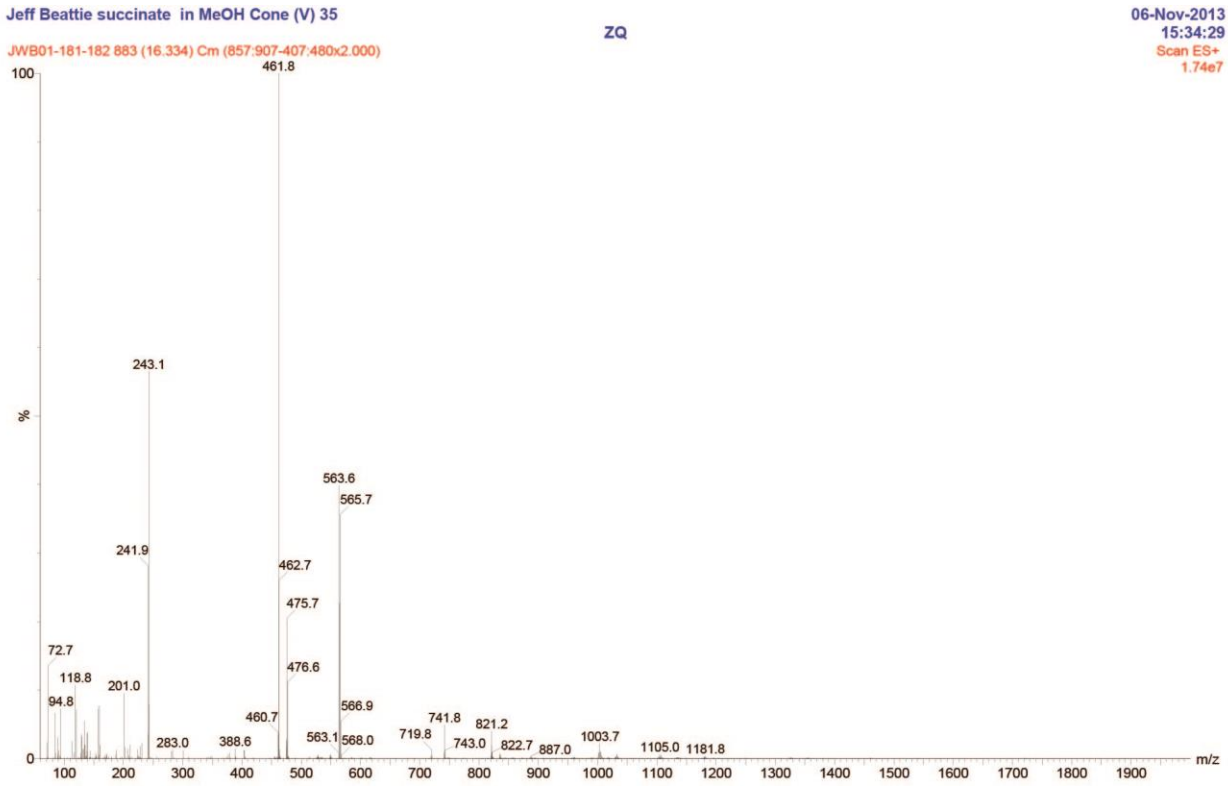

Figure S15. ESI-MS of **$Ni_2(L)Br_4$ + Succinate** and **Oxalate**

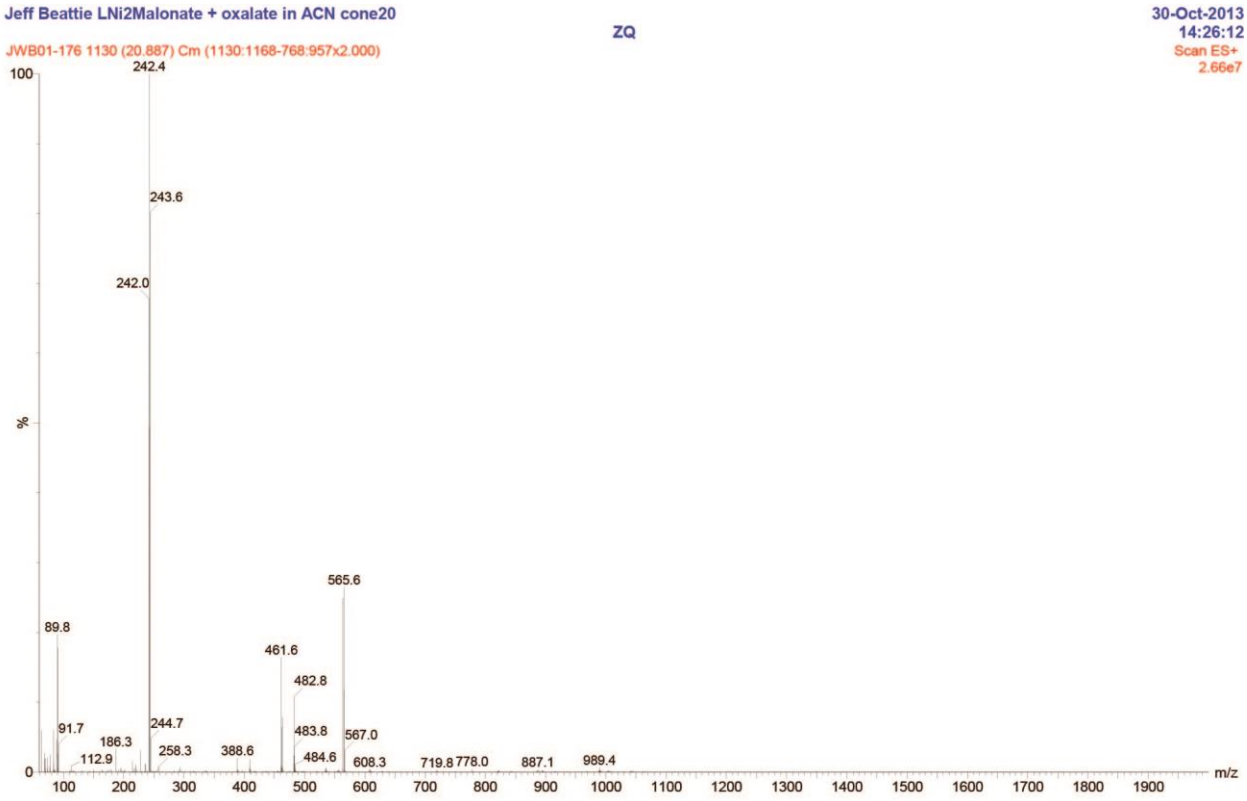

Figure S16. ESI-MS of **$Ni_2(L)Br_4$ + Glutarate** and **Oxalate**

3. X-ray crystallographic details

Structures of compounds **1, 2, 3, 4,** and **1•CaBr$_2$(THF)$_4$** were confirmed by X-ray structure determination. The crystals were mounted on a Bruker APEXII/Kappa three circle goniometer platform diffractometer equipped with an APEX-2 detector. A graphic monochromator was employed for wavelength selection of the Mo Kα radiation (λ = 0.71073 Å). The data were processed and refined using the APEX2 software. Structures were solved by direct methods in SHELXS and refined by standard difference Fourier techniques in the SHELXTL program suite (6.10 v., Sheldrick G. M., and Siemens Industrial Automation, 2000). Hydrogen atoms were placed in calculated positions using the standard riding model and refined isotropically; all other atoms were refined anisotropically. Some of the para-^{i}Pr groups displayed large wagging motion which in selected cases (**1**) was successfully modeled as two different conformations. In contrast, we had only limited success in modelling the disorder of the para-^{i}Pr groups in the structures of **2** and **3.** Even though these structures were collected at 100K the thermal parameters for some of these groups were very high. The conclusion is that these groups are not well defined and thus some were refined isotropically. The isotropic refinement of these atoms does not significantly alter the R-factor, and does not alter the conclusions of this paper in any way. Structures of **3** and **4** contained one molecule of ether solvent, and one molecule of acetonitrile in the asymmetric unit. Structure of **1•CaBr$_2$(THF)$_4$** contained one molecule of ether solvent in the asymmetric unit. The acetonitrile ligands in the structures of **2** and **3** were disordered over two positions. In addition, the structure of **2** contained acetonitrile solvent disordered over two positions in the asymmetric unit.

Table S1. Crystal and structure refinement data.

	1	**2**	**3**	**4**	**1**•$CaBr_2(THF)_4$
formula	$C_{25}H_{26}Br_2N_2Ni$	$C_{29}H_{35}Br_2CuN_5$	$C_{57}H_{68}N_7Br_2Ni_2O_4$	$C_{108}H_{134}Br_4N_8Cu_4O_9$	$C_{37}H_{57}Br_3N_2O_3CaNi$
Fw, g/mol	573.01	676.98	1208.42	2262.03	916.36
temperature	100(2) K	100(2) K	100(2) K	100(2) K	100(2) K
cryst syst	monoclinic	triclinic	triclinic	triclinic	triclinic
space group	*P2₁/c*	*P*-1	*P*-1	*P*-1	*P*-1
colour	pink	green	green	green	red
Z	4	2	2	2	2
a, Å	15.3126(2)	9.1051(5)	11.712(2)	12.8703(6)	8.8371(5)
b, Å	9.0515(1)	9.2898(5)	15.739(2))	17.2304(8)	10.2867(5)
c, Å	18.877(2)	18.974(1)	17.852(2)	25.5224(1)	23.517(1)
α, deg	90.00	98.136(3)	112.722(6)	108.311(2)	97.730(3)
β, deg	106.357(5)	99.496(3)	93.496(6)	102.265(2)	93.580(3)
γ, deg	90.00	103.440(3)	95.234(6)	91.872(2)	110.826(2)
V, A^3	2510.5(5)	1512.24(14)	3006.1(7)	5220.4(4)	1965.88(2)
d_{calcd}, g/cm^3	1.516	1.487	1.335	1.439	1.548
μ, mm^{-1}	3.969	3.390	2.005	2.394	3.709
2θ, deg	50.48	50.48	50.48	50.48	50.48
R_1[a] (all data)	0.0576	0.0615	0.0711	0.0528	0.0775
wR_2[b] (all data)	0.1077	0.1140	0.1418	0.0712	0.1221
R_1[a] [(I>2σ)]	0.0404	0.0483	0.0480	0.0329	0.0494
wR_2[b] [(I>2σ)]	0.0996	0.1090	0.1247	0.0663	0.1105
GOF (F^2)	1.093	1.371	1.061	1.051	1.017

[a] $R1 = \Sigma||F_o| - |F_c||/\Sigma|F_o|$. [b] $wR2 = (\Sigma(w(F_o^2 - F_c^2)^2)/\Sigma(w(F_o^2)^2))^{1/2}$. [c] GOF = $(\Sigma\ w(F_o^2 - F_c^2)^2/(n - p))^{1/2}$ where n is the number of data and p is the number of parameters refined.

3. UV-vis Spectroscopy

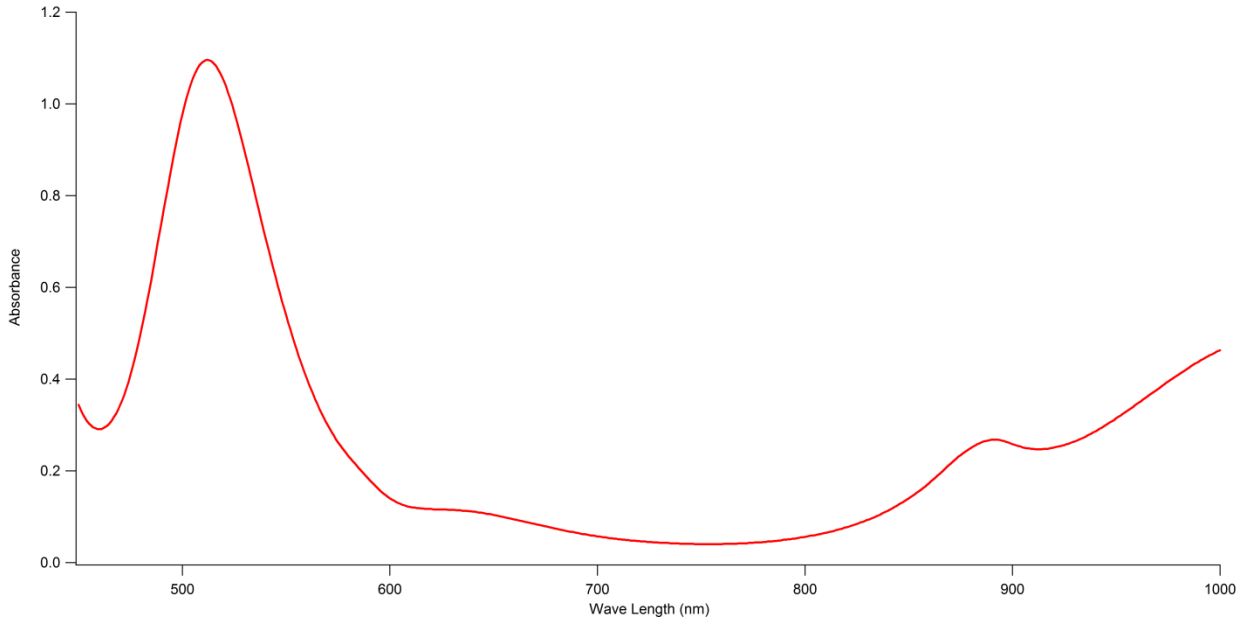

Figure S17. UV-vis spectrum of **1 (**3.5 x 10^{-6} M in THF). The spectrum was collected in the range 1000 – 450 nm.

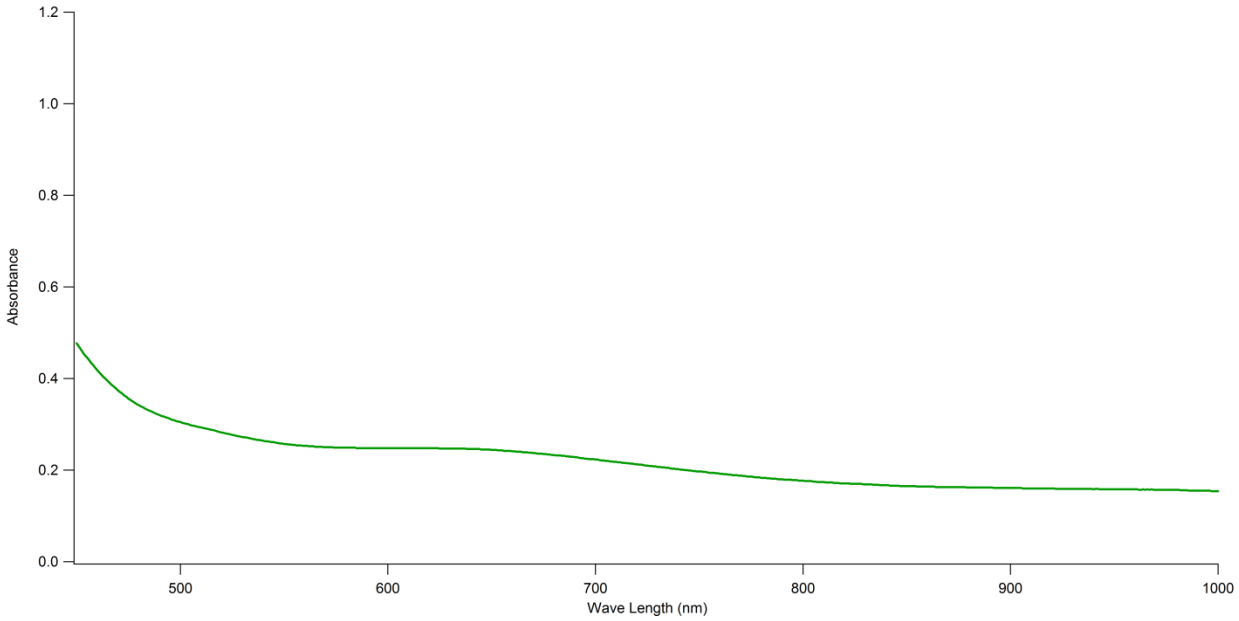

Figure S18. UV-vis spectrum of **2** (3.5 x 10^{-6} M in CH_3CN). The spectrum was collected in the range 1000 – 450 nm.

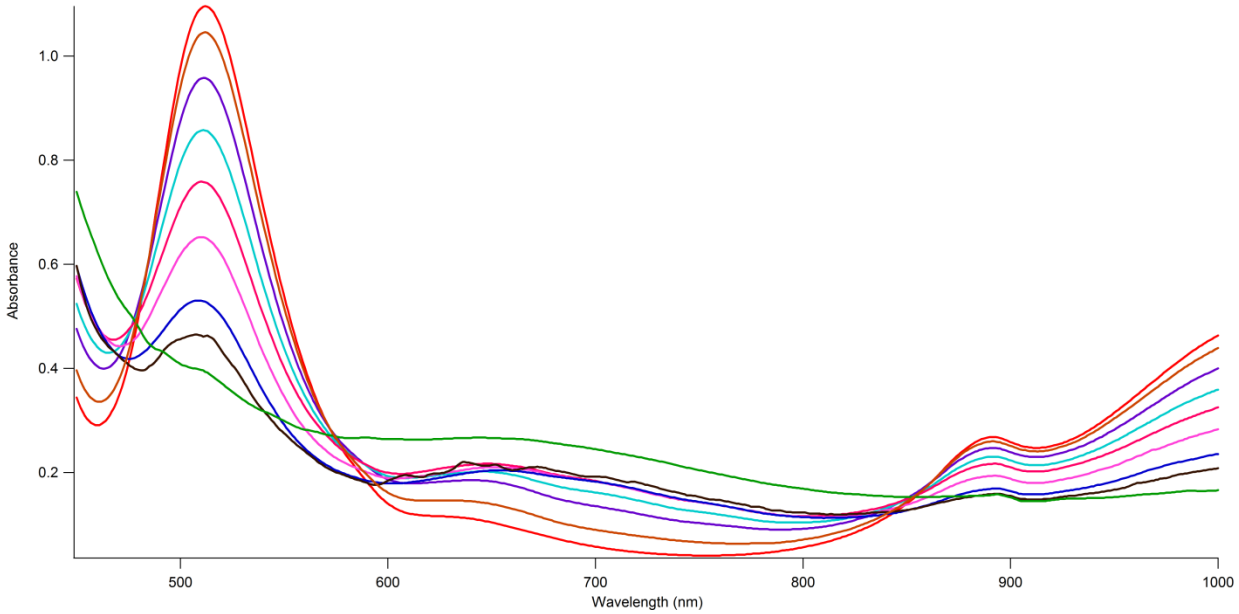

Figure S18. UV-vis spectra of the titration of **1** with **$(NBu_4)_2[C_2O_4$** To a 3 mL solution of **1 (20 mg)** inTHF 0.1 mL fractions of **(NBu4)2[C2O4]** (10 mg) in 1 mL of CH3CN were added until a stoichiometric amount was reached.

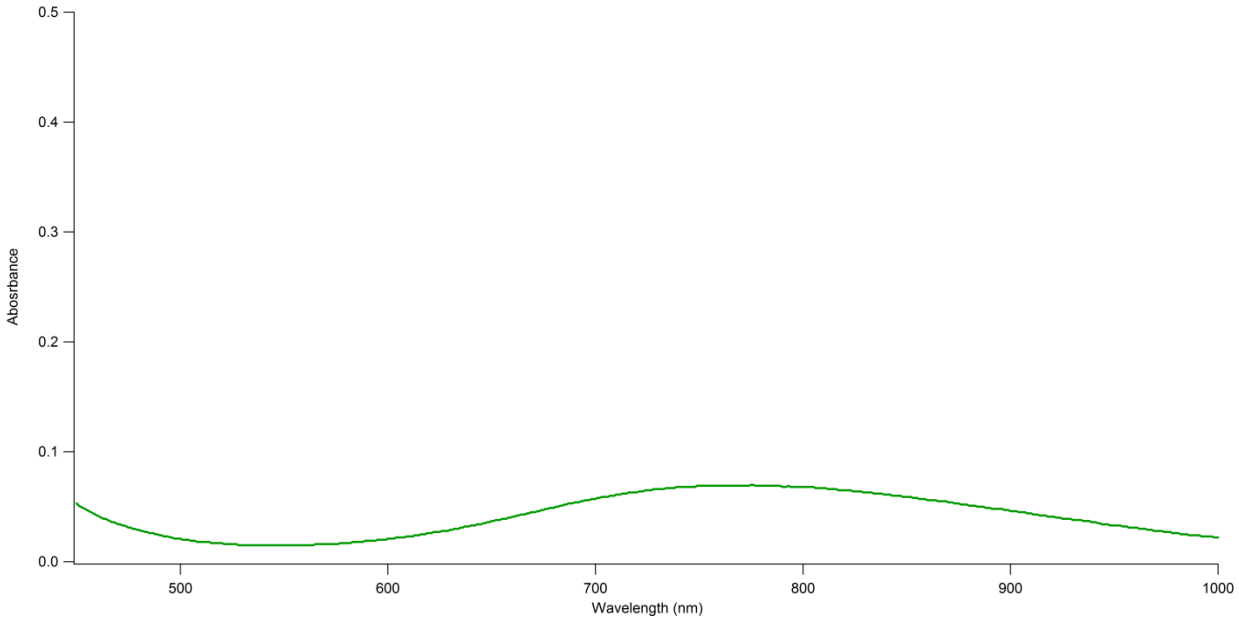

Figure S20. UV-vis spectrum of **2 (**1.7 x 10^{-6} M in CH_3CN). The spectrum was collected in the range 1000 – 450 nm.

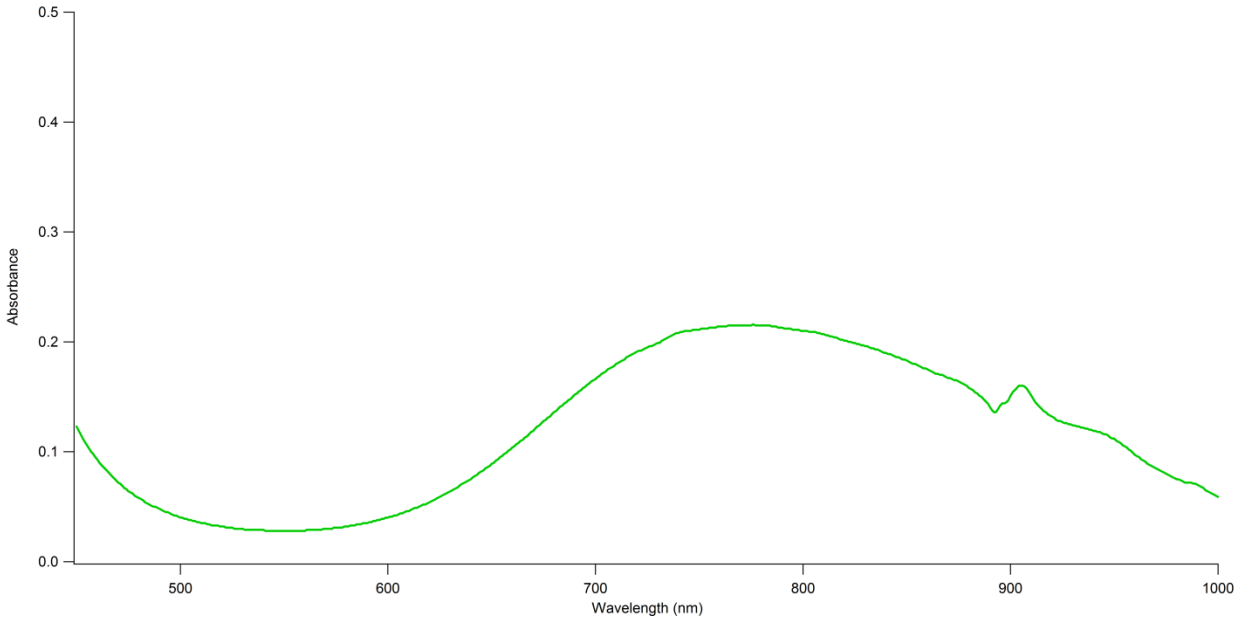

Figure S21. UV-vis spectrum of **4 (**1.7 x 10^{-6} M in CH_3CN). The spectrum was collected in the range 1000 – 450 nm.

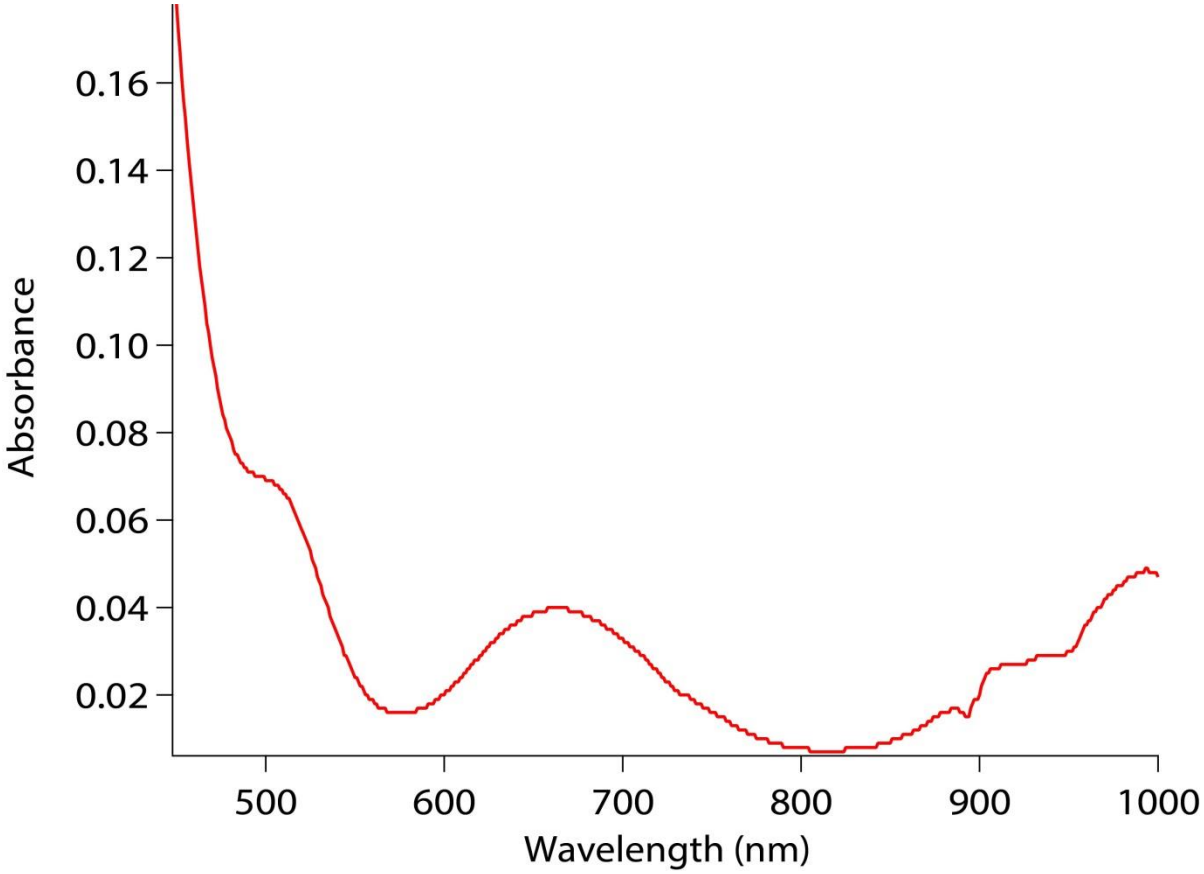

Figure S22. UV-vis spectrum of the product of the reaction between **1** and formate. The reaction was carried out by treating 1.5 mL of a 9.2 mM CH_3CN solution of 1.5 mL of a 9.2 mM CH_3CN solution of formate. The spectrum was collected in the range 1000 – 450 nm.

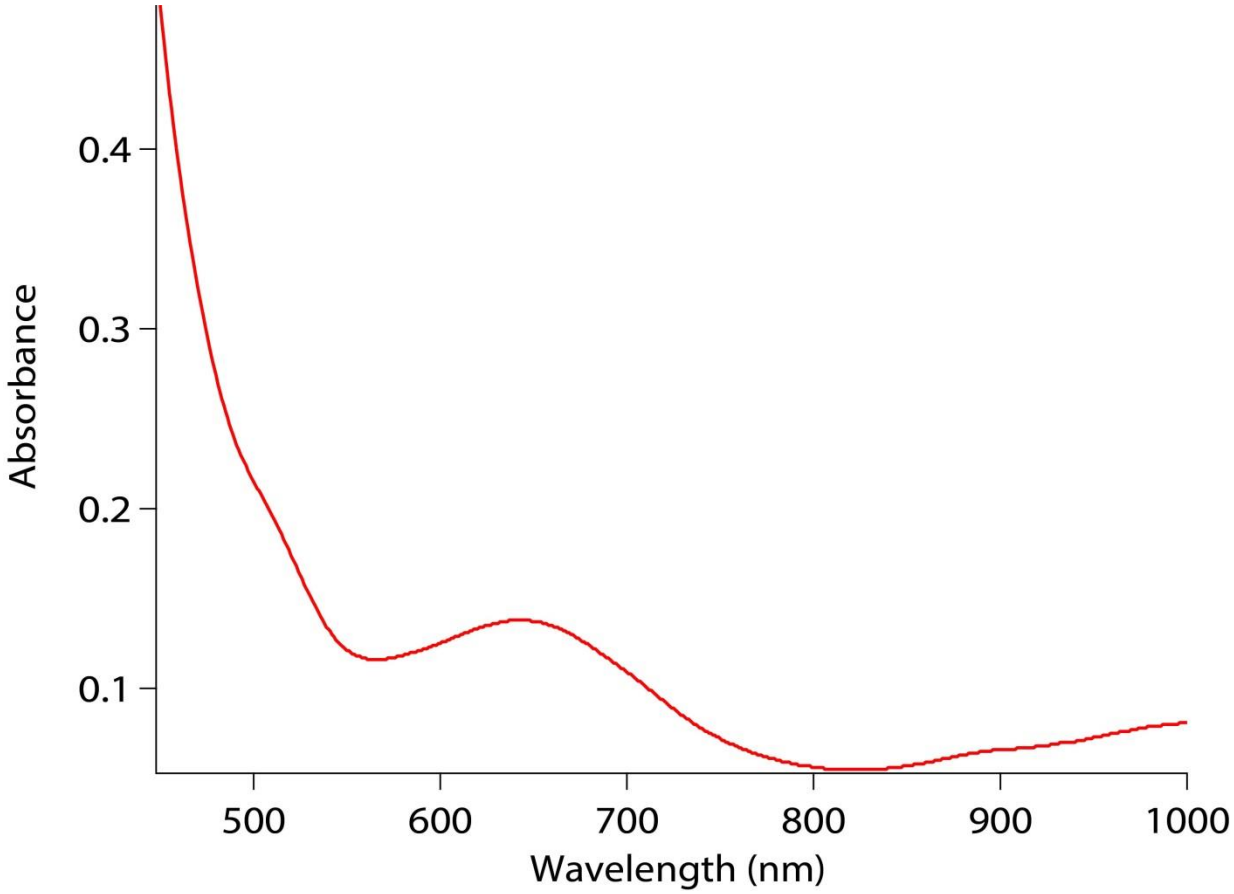

Figure S23. UV-vis spectrum of the product of the reaction between **1** and acetate. The reaction was carried out by treating 1.5 mL of a 9.2 mM CH_3CN solution of 1.5 mL of a 9.2 mM CH_3CN solution of formate. The spectrum was collected in the range 1000 – 450 nm.

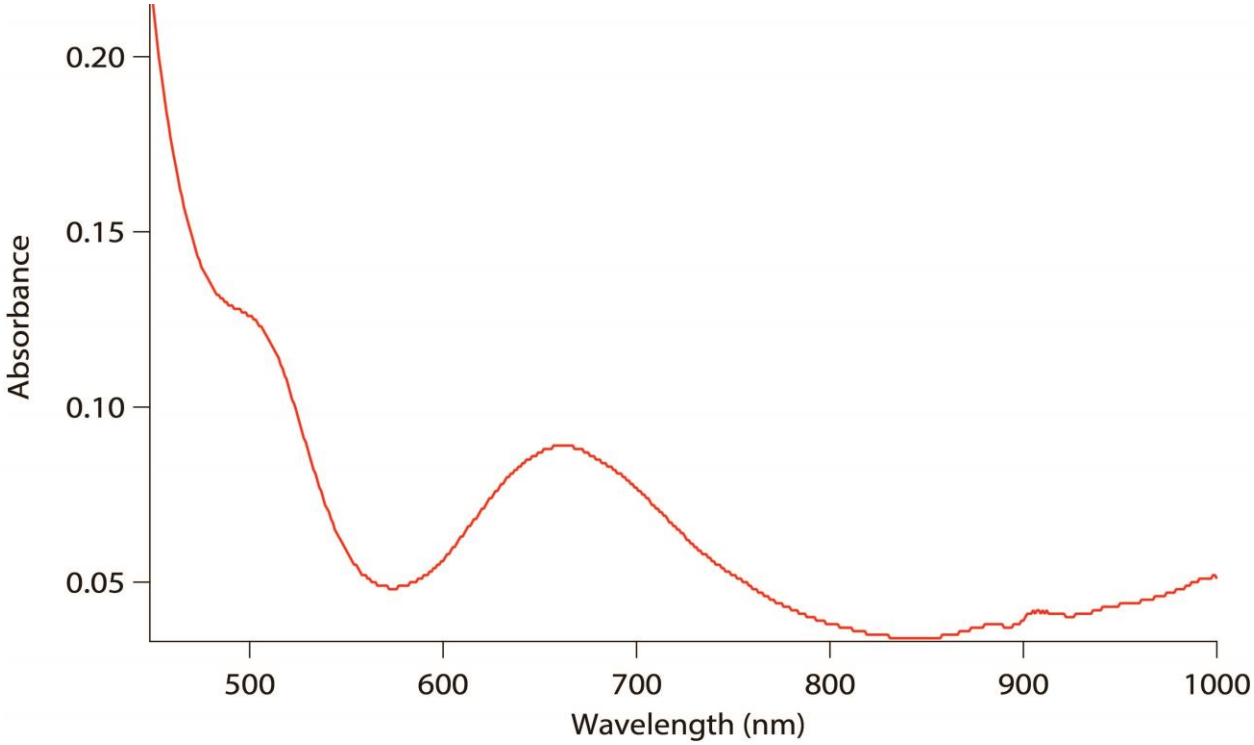

Figure S24. UV-vis spectrum of the product of the reaction between **1** and malonate. The reaction was carried out by treating 1.5 mL of a 9.2 mM CH_3CN solution of 1.5 mL of a 9.2 mM CH_3CN solution of malonate. The spectrum was collected in the range 1000 – 450 nm.

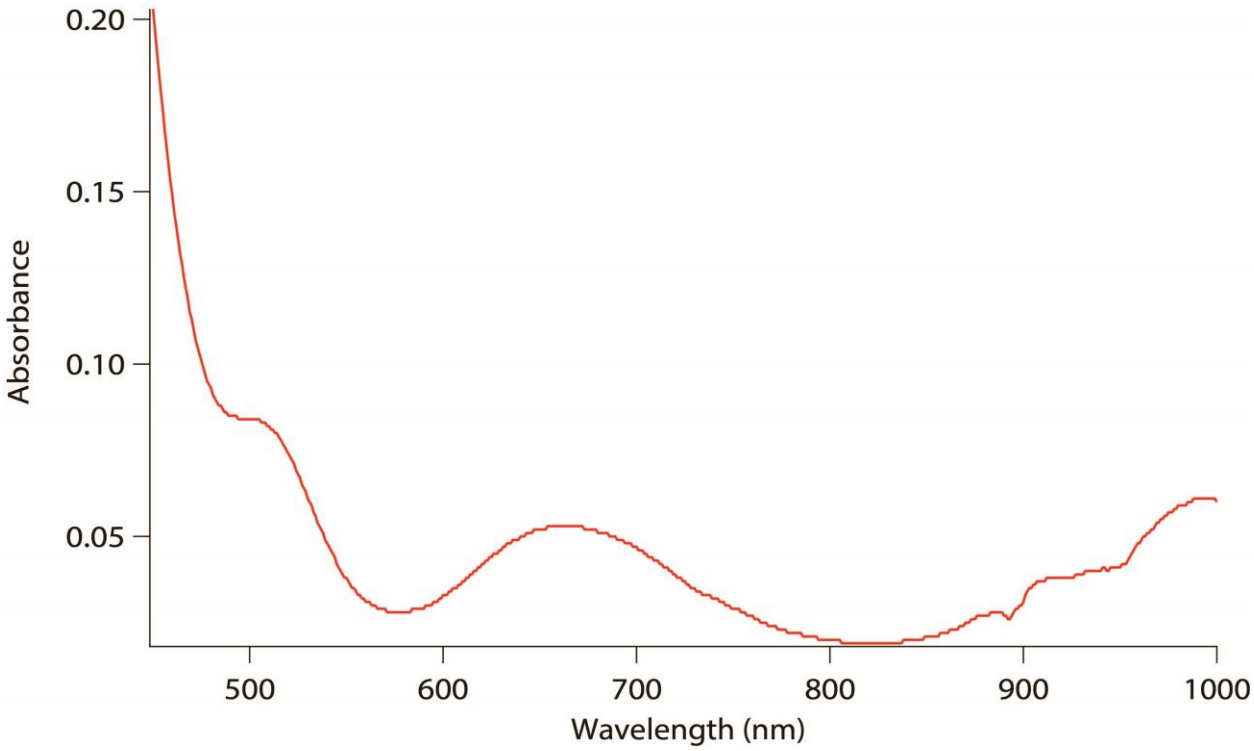

Figure S25. UV-vis spectrum of the product of the reaction between **1** and succinate. The reaction was carried out by treating 1.5 mL of a 9.2 mM CH_3CN solution of 1.5 mL of a 9.2 mM CH_3CN solution of malonate. The spectrum was collected in the range 1000 – 450 nm.

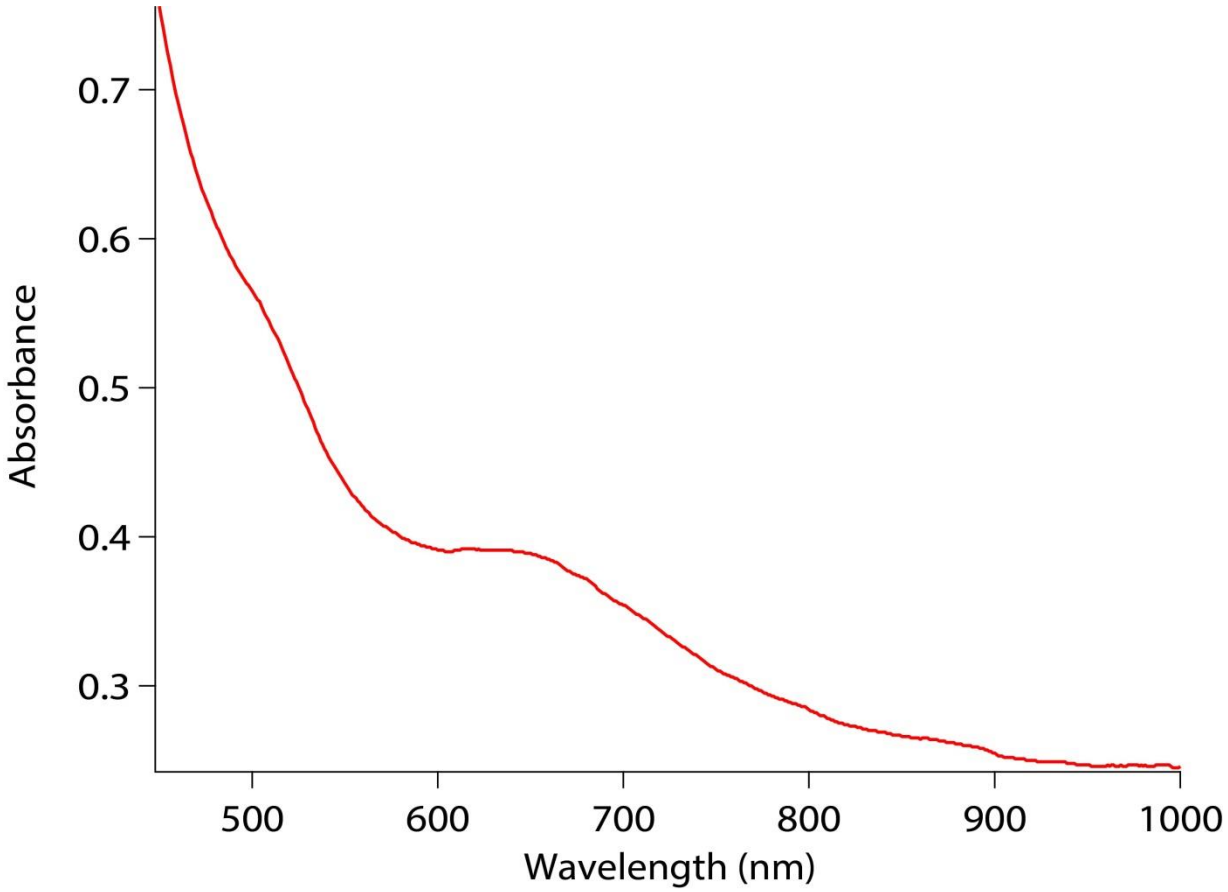

Figure S26. UV-vis spectrum of the product of the reaction between **1** and glutarate. The reaction was carried out by treating 1.5 mL of a 9.2 mM CH_3CN solution of 1.5 mL of a 9.2 mM CH_3CN solution of malonate. The spectrum was collected in the range 1000 – 450 nm.

5. Determination of Binding Constant

The stoichiometry of oxalate binding to the metal complex is 1:1 based on the mass spectrometry, X-ray crystallography, and elemental analyses. The binding constant for 1:1 binding between the donor and acceptor is determined using the equation below. [1]

$$\Delta A_{obsd} = \varepsilon_{\Delta HG} \times \frac{\left[[M] + [L] + \left(\frac{1}{K}\right) - \sqrt{\left([M] + [L] + \left(\frac{1}{K}\right)\right)^2 + 4[M][L]}\right]}{2}$$

The terms in the equation are defined below:

ΔA_{obsd} = observed change in absorption of metal complex after it is binds the ligand (oxalate)

$\varepsilon_{\Delta HG}$ = change in molar absorptivity of the metal complex with and without ligand (in our case, the difference between **1** and **3**).

[M] = Concentration of the metal complex (**1**, mM)

[L] = Concentration of the ligand (oxalate, mM)

K = binding constant

The method of UV/vis titrations has been used to determine the binding constant, K. In this method the concentration of the metal complex (**1**) was held constant (at 3.09 mM). Eight different samples were prepared with varying concentrations of the ligand (oxalate). The concentrations of the ligand used are listed in **Table S2**. The values of ΔA_{obsd} are also shown in **Table S2**.

Table S2. The UV/Vis data used to plot binding isotherms for the metal complex (**1**) and the ligand (oxalate). Concentration of metal complex was kept constant at 3.09 mM for all the samples.

Sample	[Oxalate] (mM)	$-\Delta A_{obsd}$
1	0	0
2	0.3097	0.037
3	0.6194	0.055
4	0.9291	0.105
5	1.2388	0.123
6	1.5485	0.163
7	1.8582	0.182
8	2.1679	0.191

Generally, stronger absorption is observed for the product, resulting in the positive ΔA_{obsd} values. In the present case, stronger absorption was observed for the starting material (**1**) versus the product (**3**). To account for this phenomenon, the equation was modified by multiplying by (-1) on both sides. The (ΔA_{obsd}) values were plotted against the concentration of the ligand to obtain series of data points. These points were fitted into a non-linear curve using the method of non-linear least squares and by writing a custom program using Igor software. This data analysis determined the binding constant K to be $5.2(5) * 10^2\ M^{-1}$

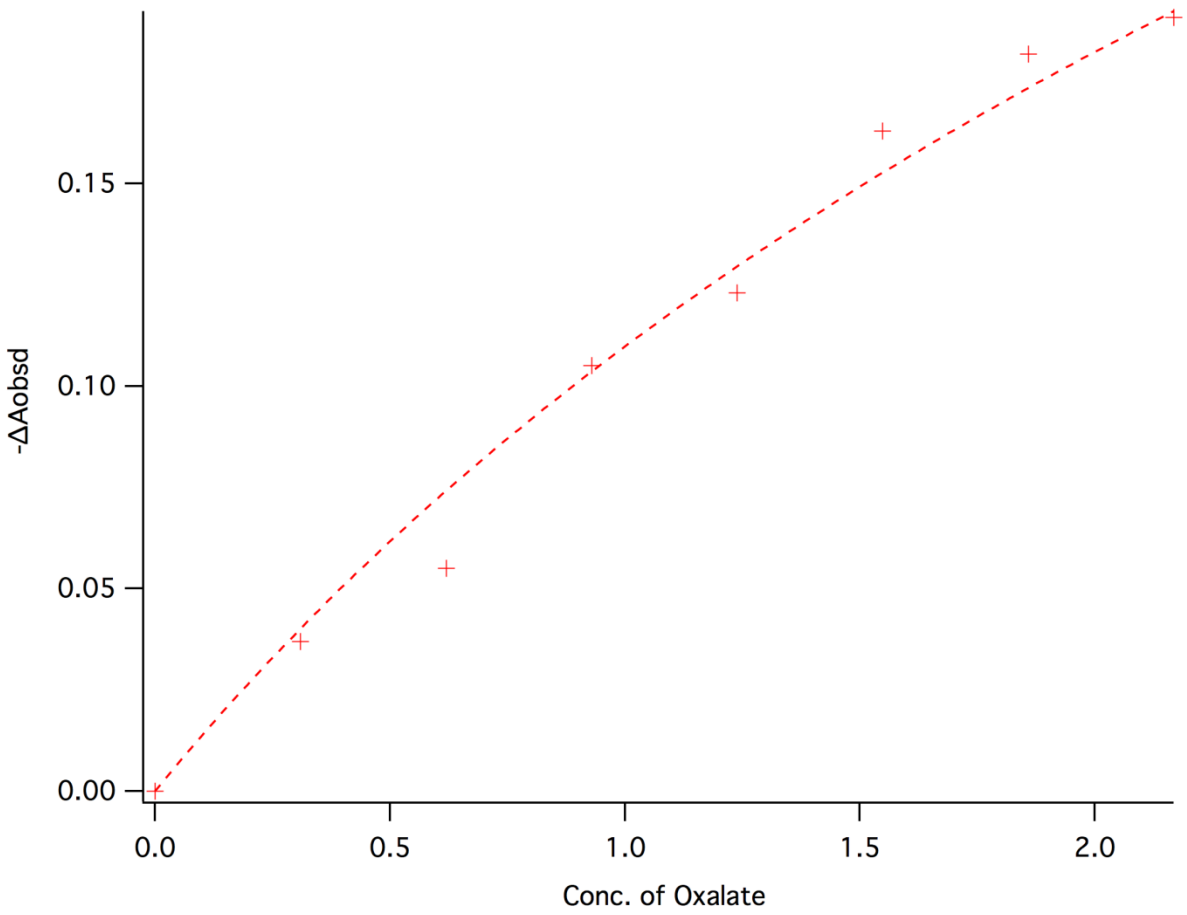

Figure S27: The binding isotherms for Metal/Ligand mixtures.

5. References

1. Pall Thordarson. Determining association constants from titration experiments in supramolecular chemistry. Chem. Soc. Rev., 2011, 40, 1305–1323.